LIMIT ANALYSIS UNDER LATERAL LOADS OF MASONRY VAULTS UPDATED BY Ω-WRAP

LAURA ANANIA and GIUSEPPE D'AGATA

Dept of Civil Engineering, University of Catania, Italy

In this paper, the structural behavior under lateral load of a masonry-barrel vault, strengthened by new technology by applied Carbon-Fiber Reinforced Polymer (C-FRP), is discussed from both theoretical and experimental points of view. The C-FRP is applied such as to assume an Ω shape around a concrete core at the vault extrados. A theoretical prediction of ultimate strength was derived in agreement with observations during the experiments (e.g., masonry crushing, FRP rupture, debonding, sliding along the mortar joint). A lower-bound limit-analysis approach was developed that can handle the shear strength of each ideal section given by the Mohr-Coulomb friction law (for the mortar joint). It can also handle other non linear Italian Code relations (for CFRP Ω-Wrap reinforcement) at a given level of normal compressive stress resulting from the previous step.

Keywords: Arch, Masonry structure, Strengthening, FRP, Experiments.

1   INTRODUCTION

The preservation of architectural heritage presents one of the most important challenges in civil engineering due to the complexity of the geometry of the structures. This is particularly important for existing constructions in the seismic area. External bonding of composites has become a popular technique for strengthening historic monumental masonry buildings (Capozucca 2007). In the case of masonry-barrel vaults, the efficiency of a strengthening system based on the use of Carbon-Fiber Reinforced Polymer (C-FRP) is due to its capability to absorb tensile stress and limit hinge formation and related collapse mechanisms.

The performance of the interface between composites and masonry is one of the key factors affecting the behavior of strengthened structures (Lourenço et al. 2006). When C-FRP strip reinforcements are applied to curved surfaces, or when the flexural stiffness of the fibers is high, it can have significant tensile stresses in a direction normal to the interface (peeling), which deplete transmissible anchoring forces. C-FRP can be applied either to extrados or inside the concrete strips, but recent studies (Anania et al. 2014) have shown their vulnerability to the shear collapse mechanism caused by peeling. In order to avoid premature collapse such as from the peeling, an innovative technology called "Ω-Wrap" has been proposed, based on the idea of shaping the composite strips to transmit sufficient stiffness. An omega-shape (Ω) positioning of the C-FRP sheets was chosen, wrapped around a high-resistance mortar core cast and molded on site.

2   THE EXPERIMENT

The barrel vault consisted of calcareous bricks 7 x 7 x 15 cm in dimension, arranged in a single sheet, with 23 rows of blocks, and bedridden with mortar of hydrated lime and cement of class M2.5 N/mm^2 according to Italian codes. The Ω-Wrap system nucleus dimensions were 5 cm in height and 10 cm in width, and cast on the extrados of the vault (Figure 1). The CFRP was placed around the core and swaged on the extrados of masonry for a width equal to 5 cm at each side. It comprised two layers of uniaxial arranged at right angles to each other, forming a balanced biaxial reinforcement with equivalent thickness of 0.167 mm in each orthogonal direction (Figure 2). Table 1 reports the main mechanical properties of the materials used, some of which were as reported in Anania et al. (2012).

The design value of the intermediate delamination tensile strength of CFRP is determined by multiplying by 3 the factors related to the overboard delamination, according to code CNR-DT200/2004 for concrete. The reinforcement should be uniformly applied along the generatrix with a suggested step given by code CNR-DT200/2004.
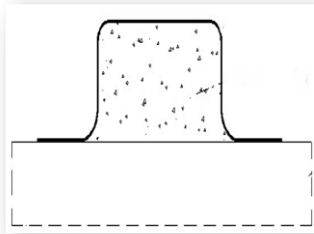
Figure 1. Ω-Wrap system.   Figure 2. Strengthened arch by Ω-Wrap system.

Table 1. Mechanical properties of the brick and mortar.

Material	Tensile Strength f_{mtm} (N/mmq)	Compressive Strength f_{mk} (N/mmq)	Young Modulus E (N/mmq)	Fracture Energy Gf (N/mmq)
Calcareous rock	1	12, 60	9. 500	0, 4
Mortar joint	0, 22	0, 69	675	0, 16
C-FRP	4. 830	0	230. 000	-
High resistance mortar	1	6	20. 000	0, 2

The model was implemented by constraining one abutment as fixed and the other as mobile. The extreme mortar joints, near the supports, were implemented by a given infinite value to the resistant shear, in order to take into account the presence, in real structures, of the walls supporting the upper floors.

The fixed abutment (Figure 3) was created by means of an L-shaped profile 120 x 80 x 8 mm welded to a steel plate directly connected to the concrete basement. The mobile abutment was created by means of a L-shaped profile 120 x 80 x 8 mm welded to a steel plate, free to slide above another steel plate 700 x 500 x 20 mm. The sliding

was provided by a proper steel profile wrapped in Teflon 0.3 mm thick (Figure 4).   On both extremities of the arch a shear restrain was performed by a C profile 150 x 80 x 5 mm as shown in Figures 3 and 4.

Figure 1. Fixed abutment.

Figure 2. Sliding abutment.

3   EXPERIMENTAL CAMPAIGN

An experimental investigation on a suite sample in a scale of 1:2 of a typical traditional one-ring masonry arch with a span of 3 m was carried out. This sample was the object of other experiment under vertical load applied to one fourth of the arch span (Anania et al. 2013). It was first repaired. The repairing technique applied to the vault consisted of cleaning the damaged surface and joints, then removing and substituting the damaged bricks, and finally filling the mortar joint cracks with special resins. The repairing technique was only to the masonry structure, while the damaged composite located between section 17-18 (Figures 5 to 6) remained unrepaired. Those sections, in fact, were the ones corresponding to the load section point in the previous experiments.

As noted above, the arch was tested by a controlled displacement applied to the mobile abutment of the arch. This was done by means of a screw jack placed in series to a load cell of 250 KN capacity, so as to simulate the action of a horizontal load. Two displacement transducers were located at the mobile abutment of the arch. Eight strain gauges are placed along the CFRP material. Figure 7 reports the arch ready for testing.

3. 1   The Experimental Collapse Mechanism

First shear crack occured at 5 kN in both the sections no. 11 and 14 at the estrados. For a load equal to 6 kN, estradosal cracks appeared at sections no. 14 and 4. Section no. 18, the one that in the previous test was the loaded section, cracked under a load of 7 kN, while even sections no. 1 and 23 exhibited damage. When the load was increased up to 8kN, intradosal hinges at the extremities of the arch (section 1-23) developed, and this produced the sliding of bricks voussoir with each other. When the load of 8kN was exceeded. cracks developed in all cases, especially in section no. 17-18 abruptly. At a load of 8.5 kN. the reinforced rib, already damaged by the previous test, was broken.

Figure 1.   Cracks on the masonry vaults *ante operam.*
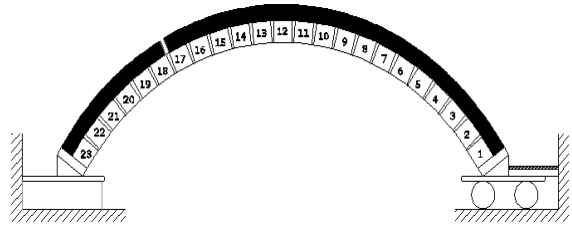
Figure 2.   Static scheme of the arch and section identification.
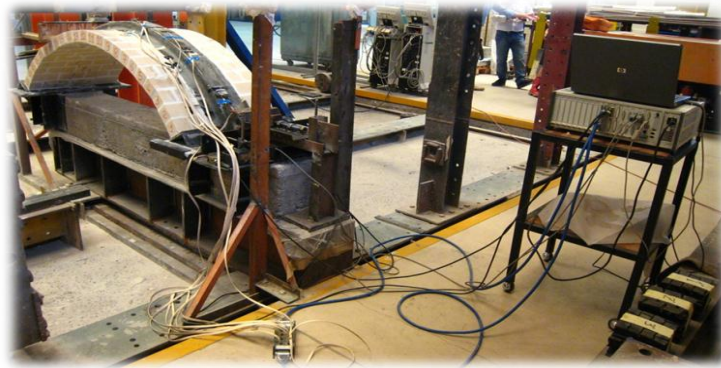
Figure 3.   The sample before the test.
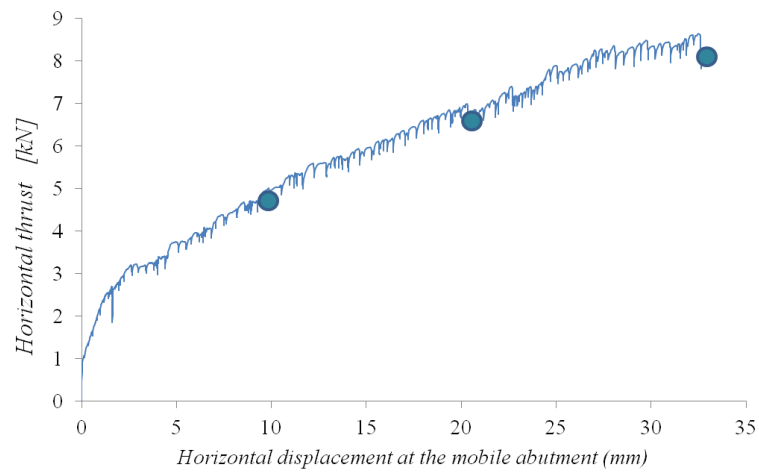
Figure 4.   Load displacement curve.
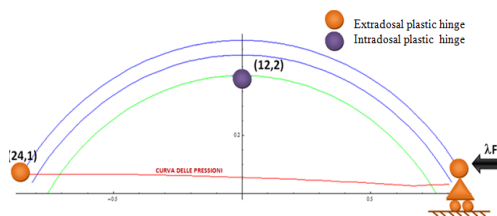
Figure 5. Theoretical collapse mechanism.

Figure 8 plots the diagram obtained by the experimental test. A loss of load can be observed each time a crack develops or a plastic hinge occurs. The collapse mechanism (Figure 9) is thus represented by the formation of three hinges: one at the extrados at section no. 1. (Figure 10), another at the intrados in section no. 23 (Figure 11), and finally one at the extrados in section no. 18 (Figure 12).

Figure 6. Sec. no. 1.   Figure 7. Sec. no. 23.   Figure 8.   Sec. no. 18.

4 LIMIT ANALYSIS

The method was based on limit analysis and used the static-theorem approach (safe – or lower-bound – and uniqueness theorems) to determine the ultimate capacity of the structures analyzed by means of an optimization process. The proposed limit-analysis formulation relies on a number of assumptions necessary for the validity of the limit theorems (Milani et al. 2009a, 2009b). For that purpose, the arch geometry is described by decomposing the entire masonry vault (or arch) in a series of equally-spaced short segments (or fictitious "voussoirs"), limited by sections oriented perpendicularly to the axis. With an appropriate choice of the three undetermined unknowns, the equations of equilibrium can be conveniently reformulated by obtaining the internal forces as a function of them, as better described in Anania et al. (2013b). In the present case, the code must consider the presence of the damage in section no. 17 by eliminating the resistance of C-FRP in that section. The extreme mortar joints near the supports were implemented by a given infinite value of the resistant shear, in order to take account of the presence, in real structures, of the walls supporting the upper floors. Besides taking into account the presence of the sliding bearing in section no. 1 (Figure 17), an appropriate M-N domain was determined. The condition $M_1=0$ and $N_1=0$ constitutes a limit condition, and the M-N domain crosses through the origin of the reference system.

With these data the collapse load $F_u = 1cF = = 8.59$ kN is obtained very close to the experimental one. Thanks to the perfect accordance between experimental and analytical data, the collapse load of the same arch can be determined also in the case of a non-damaged C-FRP in section no. 17. In that case, a collapse load equal to $F_u = 1cF = 16. 70$ kN can be obtained. Therefore it is possible to say that the damaged fiber produces a reduction of the ultimate load up to 50%.

5   CONCLUSIONS

The comparison between the theoretical and experimental data exhibits a good agreement also in terms of damage evolution. Thus, we can confirm that the proposed analytical procedure is able to highlight all the capability of the new strengthening technique even in the case of horizontal actions. Again, the proposed system shows the capability of the composite of working in compression without any unsuitable buckling effect. thanks both to its curve shell shape and to the adherence between a good substrate and composite. Overall, the proposed technology seems to be very attractive thanks to its capability of transferring horizontal seismic actions to masonry walls. In fact, the collapse mechanism avoids both global and local crashes of the vault due to the bearing capacity of the ribbed roof.

References

Anania, L., Badalà, A., and D'Agata, G., Bond behavior of standard and reinforced anchorage between CFRP sheet and natural calcareous stone, *Applied Mechanics and Materials* (446-447), 1091-1098, 2014.

Anania, L., Badala, A., and D'agata, G., Experimental validation of an algorithm for the reinforced masonry vaults by ω-wrap technique, *Earthquake Resistant Engineering Structures IX*, WIT Transactions on The Built Environment (132), 297-308, 2013.

Anania, L., Badalà, A., Barone, G., Belfiore, C. M., Calabrò, C., La Russa, M., Mazzoleni, P., and Pezzino, A., The stones in monumental masonry buildings of the "Val di Noto" area: New data on the relationships between petrographic characters and physical-mechanical properties *Construction and Building Materials*, Elsevier Vol. 33C, 122-132, 2012.

Capozucca, R., Behavior of CFRP sheets bonded to historical masonry, *Proceedings of the Asia–Pacific Conference FRP in Structures*, Hong Kong, 723–8, 2007.

CNR-DT 200/2004, Instructions for design, execution and control of the structural retrofit by means of the use of composite materials of the R.C., pre-stressed R.C. and masonry structures, 2004.

Lourenço, P. B., and Oliveira, D. V., Strengthening of masonry arch bridges: research and applications, *Proceedings of the First International Conference on Advances in Bridge Engineering, Bridges - Past, Present and Future*, Brunel University, West London, 26-28th June 2006.

Milani, E., Milani, E., and Tralli, A., Upper bound limit analysis model for FRP-reinforced masonry curved structures. Part II: Structural analyses, *Computers and Structures* 87, 1534–1558, 2009b.

Milani, G., Milani, E., and Tralli, A., Upper bound limit analysis model for FRP-reinforced masonry curved structures. Part I: Unreinforced masonry failure surfaces, *Computers and Structures* 87, 1516–1533, 2009a.